

# Supporting Information

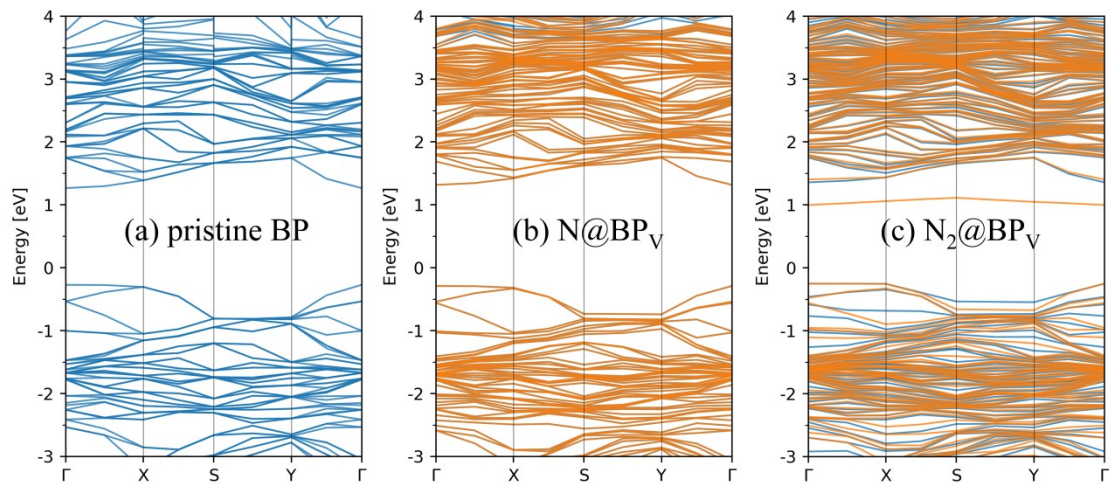
## Efficient photoreduction of carbon dioxide to ethanol on diatomic nitrogen-doped black phosphorus

Jianhua Fan, Xin Wang\*, Jing Ma, Xingman Liu, Xiaoyong Lai, Hongqiang Xia and  
Yingtao Liu\*

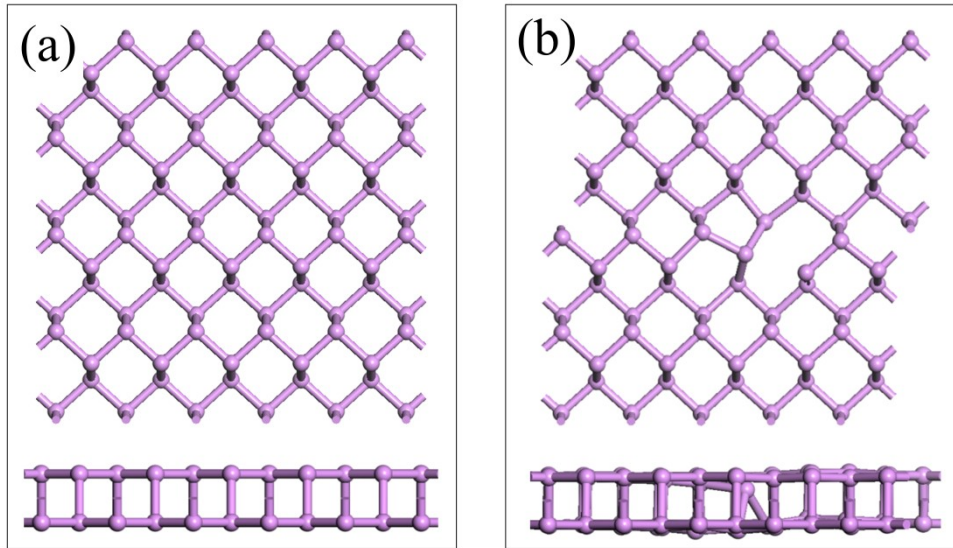
State Key Laboratory of High-Efficiency Utilization of Coal and Green Chemical  
Engineering, National Demonstration Center for Experimental Chemistry Education,  
College of Chemistry and Chemical Engineering, Ningxia University, Yinchuan  
750021, China

\*Corresponding author.

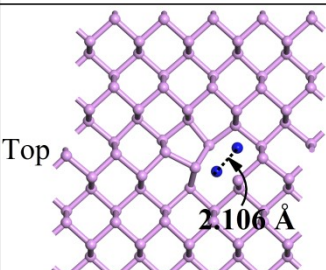
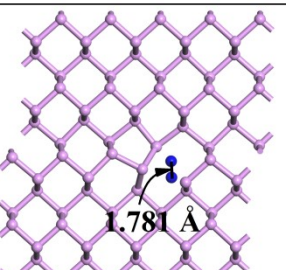
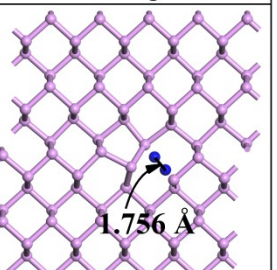
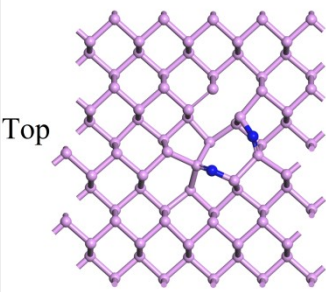
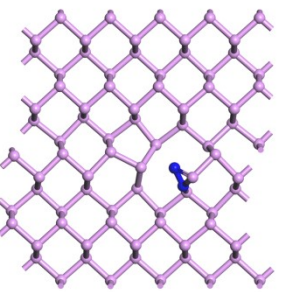
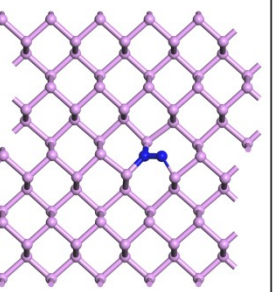
*E-mail address:* [wangxin@nxu.edu.cn](mailto:wangxin@nxu.edu.cn) (X., Wang). [liuyt@nxu.edu.cn](mailto:liuyt@nxu.edu.cn) (Y. T., Liu).



**Fig. S1.** Band structure of (a) pristine BP, (b) N@BP<sub>V</sub> and (c) N<sub>2</sub>@BP<sub>V</sub>.



**Fig. S2.** Top and side views of (a) pristine BP and (b) monatomic defective BP.

|                    | Horizontal                                                                        | Vertical                                                                           | Oblique                                                                             |
|--------------------|-----------------------------------------------------------------------------------|------------------------------------------------------------------------------------|-------------------------------------------------------------------------------------|
| Initial structure  |  |  |  |
|                    | Side                                                                              | Side                                                                               | Side                                                                                |
| Optimize structure |  |  |  |
| Formation energy   | -8.82 eV                                                                          | -7.67 eV                                                                           | -9.32 eV                                                                            |

**Fig. S3.** Initial and optimized structures of  $\text{N}_2@\text{BPV}$  in three different diatomic nitrogen-doped modes, as well as corresponding formation energy values.

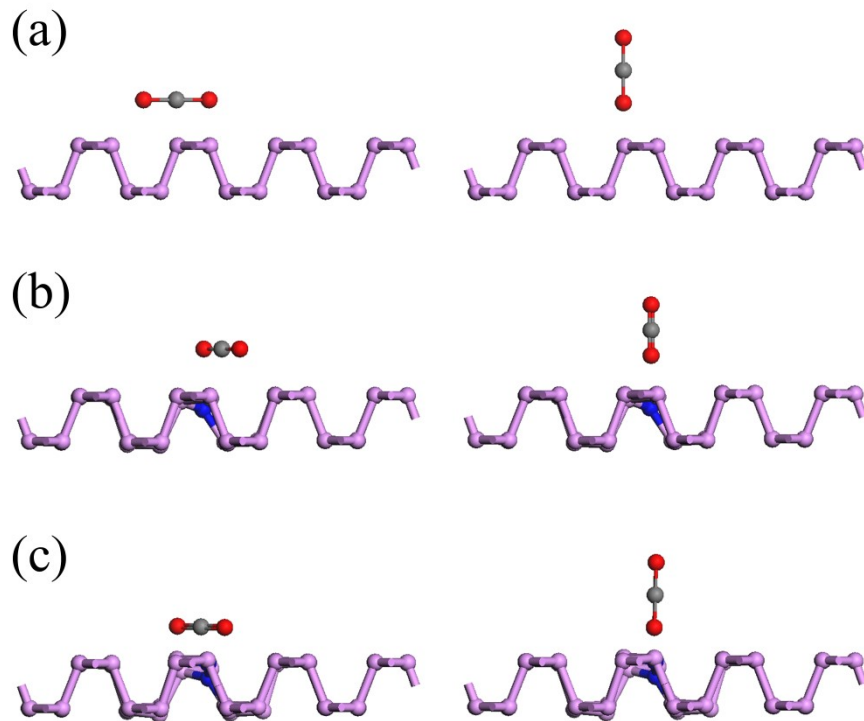


**Fig. S4.** Initial adsorption configuration of  $\text{CO}_2$  in horizontal (left) and vertical (right) directions (a) pristine BP, (b)  $\text{N}@\text{BP}_\text{V}$ , and (c)  $\text{N}_2@\text{BP}_\text{V}$ .

**Table S1** Configurations of reaction intermediate of  $\text{CO}_2$  reduction to  $^*\text{COCO}$ .

|                                 | $^*\text{CO}_2$ | $^*\text{COOH}$ | $^*\text{OCHO}$ | $^*\text{CO}$ | $^*\text{COCO}$ |
|---------------------------------|-----------------|-----------------|-----------------|---------------|-----------------|
| pristine BP                     |                 |                 |                 |               |                 |
| $\text{N}@\text{BP}_\text{V}$   |                 |                 |                 |               |                 |
| $\text{N}_2@\text{BP}_\text{V}$ |                 |                 |                 |               |                 |

**Table S2** Required gas phase properties.

| Gas molecule                          | ZPE/eV | S/eV  | TS/eV |
|---------------------------------------|--------|-------|-------|
| H <sub>2</sub> (g)                    | 0.26   | 0.001 | 0.20  |
| H <sub>2</sub> O(g)                   | 0.56   | 0.001 | 0.25  |
| CO <sub>2</sub> (g)                   | 0.30   | 0.001 | 0.66  |
| CO(g)                                 | 0.13   | 0.002 | 0.61  |
| CH <sub>3</sub> CH <sub>2</sub> OH(g) | 2.12   | 0.003 | 0.90  |
| CH <sub>3</sub> CHO(g)                | 1.46   | 0.003 | 0.81  |
| CH <sub>2</sub> CH <sub>2</sub> (g)   | 1.35   | 0.001 | 0.17  |

**Table S3** Energy (eV) of the pristine BP surface and corresponding groups.

| pristine BP | *COOH   | *OCHO   | *CO     | * + CO  | *COCO |
|-------------|---------|---------|---------|---------|-------|
| E/eV        | -460.77 | -460.91 | -451.17 | -436.33 | ----  |
| ZEP/eV      | 0.54    | 0.50    | 0.14    | 0.00    | ----  |
| TS/eV       | 0.20    | 0.13    | 0.19    | 0.00    | ----  |
| G/eV        | -460.43 | -460.55 | -451.22 | -436.33 | ----  |
| ΔG/eV       | 2.33    | 2.20    | -1.32   | -0.36   | ----  |

**Table S4** Energy (eV) of the N@BP<sub>V</sub> surface and corresponding groups.

| N@BP <sub>V</sub> | *COOH   | *OCHO   | *CO     | * + CO  | *COCO   |
|-------------------|---------|---------|---------|---------|---------|
| E/eV              | -463.06 | -464.03 | -453.40 | -438.49 | -467.26 |
| ZEP/eV            | 0.54    | 0.48    | 0.14    | 0.00    | 0.37    |
| TS/eV             | 0.26    | 0.23    | 0.19    | 0.00    | 0.29    |
| G/eV              | -462.77 | -463.66 | -453.44 | -438.49 | -467.18 |
| ΔG/eV             | 2.05    | 1.16    | -1.19   | -0.30   | 1.52    |

**Table S5** Energy (eV) of the N<sub>2</sub>@BP surface and corresponding groups.

| N <sub>2</sub> @BP <sub>V</sub> | *COOH   | *OCHO   | *CO     | * + CO  | *COCO   |
|---------------------------------|---------|---------|---------|---------|---------|
| E/eV                            | -472.50 | -472.50 | -460.01 | -444.79 | -475.78 |
| ZEP/eV                          | 0.67    | 0.67    | 0.22    | 0.00    | 0.47    |
| TS/eV                           | 0.18    | 0.18    | 0.12    | 0.00    | 0.22    |
| G/eV                            | -472.01 | -472.01 | -459.92 | -444.79 | -475.52 |
| ΔG/eV                           | -0.89   | -0.89   | 1.58    | -0.12   | -0.35   |

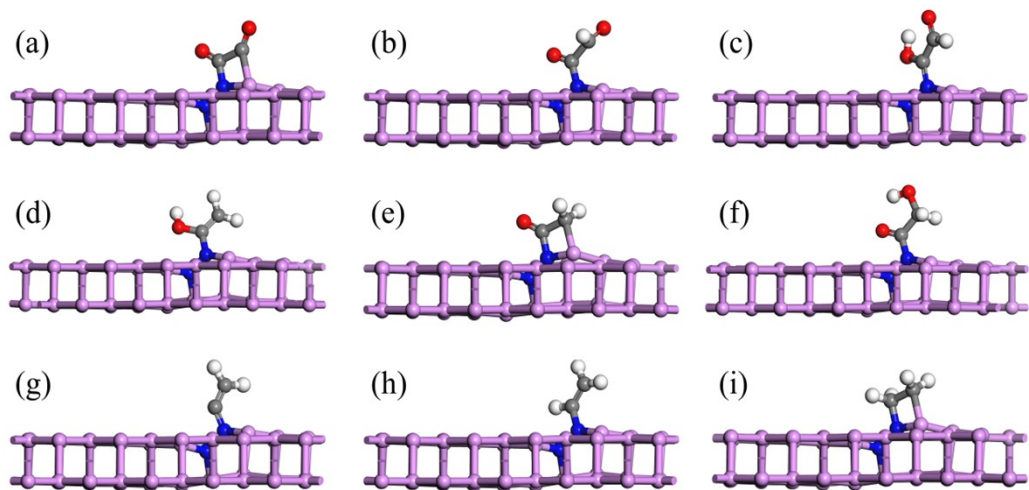


**Fig. S5.** The geometric structures during the overall reaction pathway of \*COCO conversion to  $\text{CH}_2\text{CH}_2$ : (a) \*COCO; (b) \*COCHO; (c) \*COHCHO; (d) \* $\text{COCH}_2\text{OH}$ ; (e) \* $\text{COCH}_2$ ; (f) \* $\text{COHCH}_2$ ; (g) \* $\text{CCH}_2$ ; (h) \* $\text{CHCH}_2$ ; (i) \* $\text{CH}_2\text{CH}_2$ .

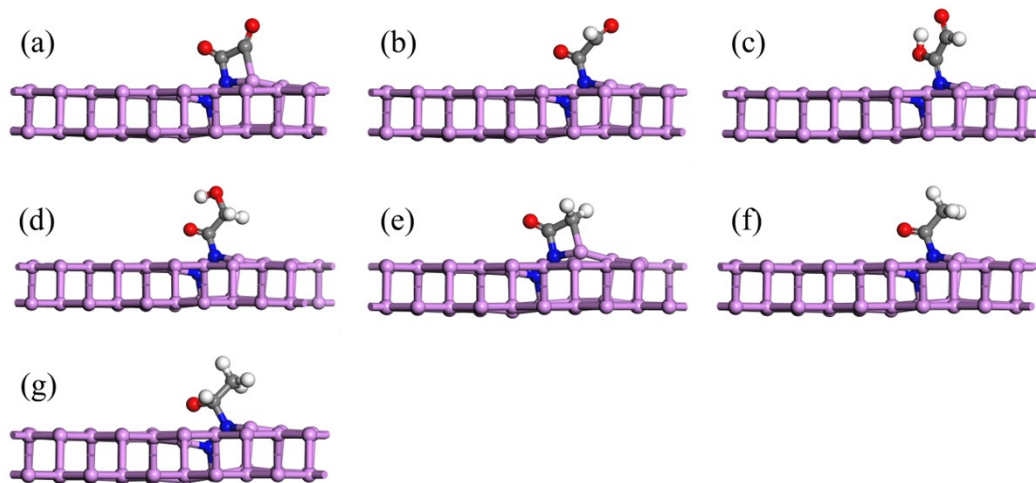


**Fig. S6.** The geometric structures during the overall reaction pathway of \*COCO conversion to  $\text{CH}_3\text{CHO}$ : (a) \*COCO; (b) \*COCHO; (c) \*COHCHO; (d) \* $\text{COCH}_2\text{OH}$ ; (e) \* $\text{COCH}_2$ ; (f) \* $\text{COCH}_3$ ; (g) \* $\text{CH}_3\text{CHO}$ .

**Table S6** Energy of CH<sub>3</sub>CH<sub>2</sub>OH, CH<sub>2</sub>CH<sub>2</sub> and CH<sub>3</sub>CHO obtained from \*COCO on N<sub>2</sub>@BP<sub>V</sub>. The red indicates a competitive path.

| species                            | E/eV                                 | ZEP/eV      | TS/eV       | G/eV           | ΔG/eV       |       |
|------------------------------------|--------------------------------------|-------------|-------------|----------------|-------------|-------|
| *COCO                              | -475.78                              | 0.47        | 0.22        | -475.52        | -0.35       |       |
| *COCHO                             | -480.18                              | 0.75        | 0.22        | -479.65        | -0.74       |       |
| <b>*COCOH</b>                      | <b>-479.28</b>                       | <b>0.75</b> | <b>0.22</b> | <b>-478.75</b> | <b>0.17</b> |       |
| *COHCHO                            | -483.55                              | 1.07        | 0.26        | -482.74        | 0.30        |       |
| *COCH <sub>2</sub> OH              | -488.46                              | 1.40        | 0.28        | -487.35        | -1.21       |       |
| <b>*COHCH<sub>2</sub>OH</b>        | <b>-490.92</b>                       | <b>1.72</b> | <b>0.23</b> | <b>-489.43</b> | <b>1.31</b> |       |
| <b>*CHOCH<sub>2</sub>OH</b>        | <b>-490.21</b>                       | <b>1.72</b> | <b>0.23</b> | <b>-488.72</b> | <b>2.02</b> |       |
| *COCH <sub>2</sub>                 | -477.25                              | 0.98        | 0.15        | -476.42        | 0.40        |       |
| CH <sub>3</sub> CH <sub>2</sub> OH | *COCH <sub>3</sub>                   | -482.09     | 1.26        | 0.24           | -481.07     | -1.25 |
|                                    | *COHCH <sub>3</sub>                  | -484.44     | 1.58        | 0.22           | -483.08     | 1.38  |
|                                    | *CHOHCH <sub>3</sub>                 | -489.20     | 1.88        | 0.24           | -487.56     | -1.10 |
|                                    | *CH <sub>2</sub> OHCH <sub>3</sub>   | -491.97     | 2.12        | 0.25           | -490.10     | 0.86  |
|                                    | *+CH <sub>3</sub> CH <sub>2</sub> OH | -444.79     | 0.00        | 0.00           | -444.79     | -0.40 |
| CH <sub>2</sub> CH <sub>2</sub>    | *COHCH <sub>2</sub>                  | -481.00     | 1.26        | 0.21           | -479.95     | -0.14 |
|                                    | *CCH <sub>2</sub>                    | -468.63     | 0.80        | 0.16           | -467.98     | 1.45  |
|                                    | *CHCH <sub>2</sub>                   | -474.35     | 1.15        | 0.16           | -473.36     | -1.99 |
|                                    | *CH <sub>2</sub> CH <sub>2</sub>     | -477.65     | 1.49        | 0.11           | -476.27     | 0.48  |
|                                    | *+CH <sub>2</sub> CH <sub>2</sub>    | -444.79     | 0.00        | 0.00           | -444.79     | 0.69  |
| CH <sub>3</sub> CHO                | *COCH <sub>3</sub>                   | -482.09     | 1.26        | 0.24           | -481.07     | -1.25 |
|                                    | *CHOCH <sub>3</sub>                  | -483.84     | 1.51        | 0.23           | -482.55     | 1.90  |
|                                    | *+CH <sub>3</sub> CHO                | -444.79     | 0.00        | 0.00           | -444.79     | -0.73 |

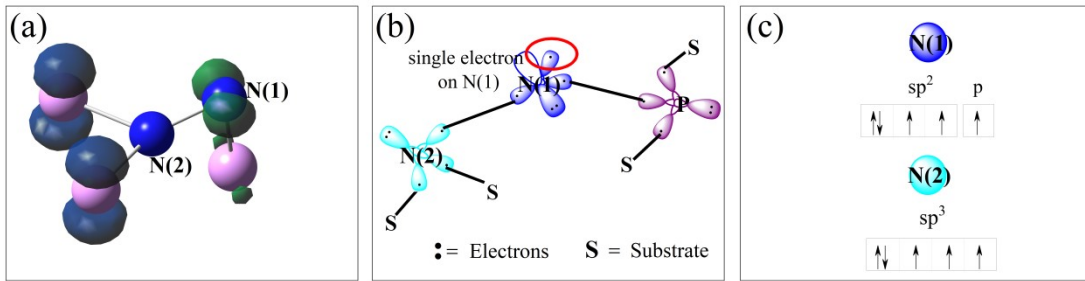


**Fig. S7.** (a) Local atomic spin population of diatomic nitrogen-doped black phosphorus (N(1) and N(2)) are used to distinguish the different N atoms. (b) Schematic of activity mechanism of N(1) atom. (c) The hybrid types of different N atoms.

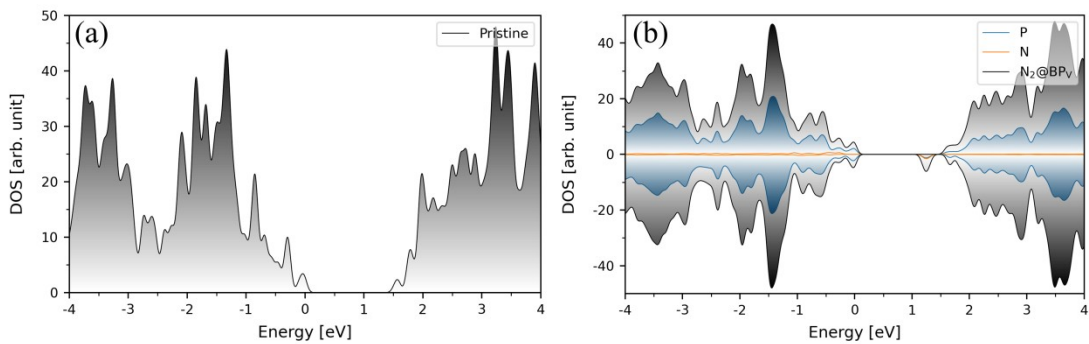


**Fig. S8.** Density of states on (a) pristine BP and (b)  $N_2@BP_V$ . DOS was obtained by the Heyd–Scuseria–Ernzerhof (HSE) functional.

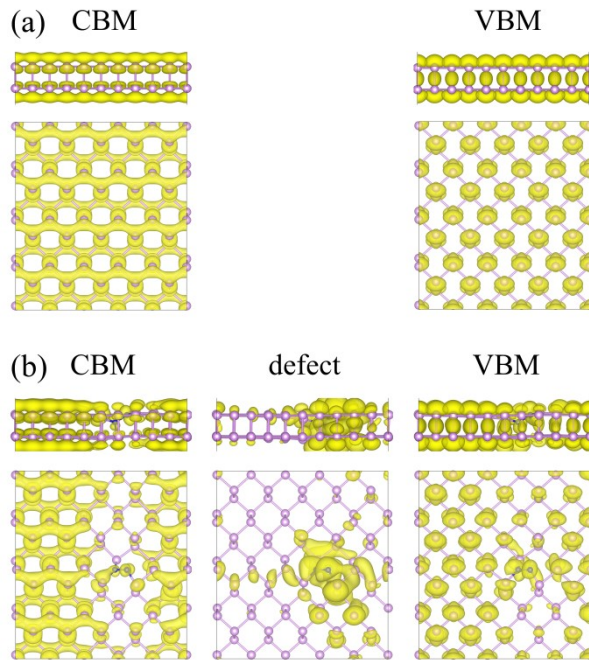


**Fig. S9.** Top and side views of the charge densities (a) pristine BP and (b)  $\text{N}_2@\text{BP}_\text{V}$ . The isosurface value is set to  $0.0004 \text{ e}/\text{bohr}^3$ .

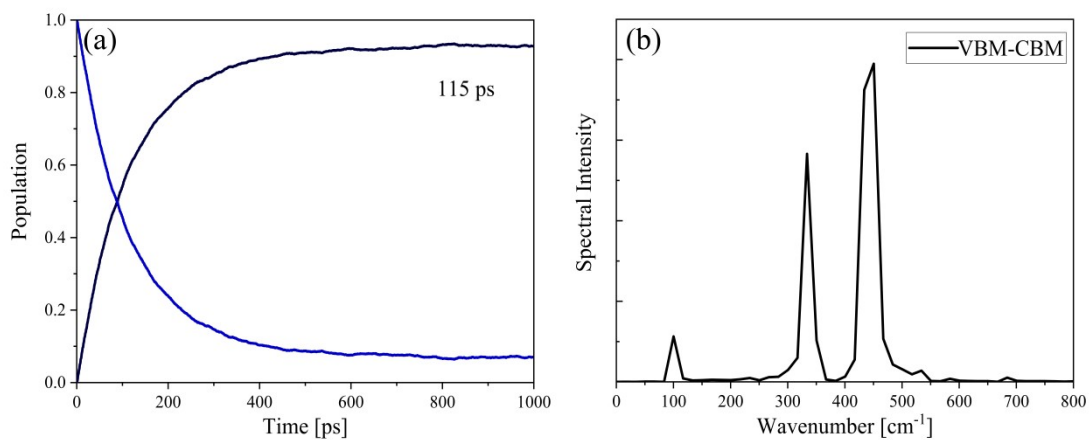


**Fig. S10.** (a)  $e\text{-}h$  recombination dynamics. The initial state corresponds to the electron excitation from the VBM to the CBM. Populations of the excited and ground are shown by the blue and black, respectively. (b) Fourier transform (FT) phonon-induced fluctuations of the energy gaps between the VBM and CBM.